

Field-induced transition in the paramagnetic state of $(\text{Sm}_{0.65}\text{Sr}_{0.35})\text{MnO}_3$ associated with magnetic clusters

R. P. Borges, F. Ott, R. M. Thomas, V. Skumryev, and J. M. D. Coey
Department of Physics, Trinity College, Dublin 2, Ireland

J. I. Arnaudas

Laboratorio de Magnetismo, DFMC & ICMA, Universidad de Zaragoza & CSIC, 50009 Zaragoza, Spain

L. Ranno

Laboratoire Louis Néel, Grenoble Cedex, France

(Received 1 February 1999; revised manuscript received 9 June 1999)

The susceptibility of $(\text{Sm}_{0.65}\text{Sr}_{0.35})\text{MnO}_3$ shows an unusual temperature dependence above the Curie temperature which is attributed to the presence of small manganese-ion clusters with $S \approx 9$. A field-induced transition is observed in the paramagnetic state, which corresponds to a doubling of the cluster size and an increase of the strength of the interaction between them. The continuous transition from small to large clusters is interpreted in terms of electron phase segregation in a two-phase region. Magnetic hysteresis in the paramagnetic state is ascribed to potential fluctuations due to Sr substitution. Magnetoresistance measurements correlate with the magnetic measurements by showing a change of regime from quadratic to linear in field when the magnetic transition is induced. Thermal hysteresis of about 8 K in the magnetization and resistivity around the Curie temperature ($T_C = 120$ K) is also related to the existence of the two paramagnetic phases. [S0163-1829(99)07741-3]

I. INTRODUCTION

There has been great interest in mixed-valence manganese perovskites following the observation of large negative magnetoresistance in these materials.¹ The main mechanism controlling the magnetic and electronic properties is double exchange, where the magnetic coupling between neighboring Mn^{3+} and Mn^{4+} ions is mediated through the transfer of an electron with spin memory. However, the crystal lattice also plays a role in this phenomenon through the Jahn-Teller distortion associated with the Mn^{3+} ion, which is static in the orbitally ordered end member LaMnO_3 and becomes dynamic in the ferromagnetic composition range where 20–40% of La is replaced by a divalent atom.

A whole range of interesting physical phenomena has been observed in the mixed-valence manganites including charge ordering, electronic phase separation,² and the existence of magnetic polarons.^{3,4} More recently some of the insulating mixed-valence manganites revealed very surprising properties. This is the case of $(\text{Pr}_{0.7}\text{Ca}_{0.3})\text{MnO}_3$, which has a partly charge-ordered ground state which may be ‘‘melted’’ to the normal metallic ferromagnetic state at low temperature by (a) applying a magnetic field greater than 6 T, (b) applying pressure, (c) irradiating with x rays, or (d) irradiating with UV light.⁵

The $(R_{1-x}\text{Sr}_x)\text{MnO}_3$ compounds with $R = \text{Sm}$ are a limiting case in the sense that the Sm ion is the smallest single rare-earth ion to form the compound with $x \approx 0.3$. The tolerance factor $t = (r_A + r_O) / \sqrt{2}(r_B + r_O)$, where r_A and r_B are the radii of the A- and B-site cations and $r_O = 1.40 \text{ \AA}$ is the oxygen radius, is equal to 0.950. The small value of t results in a pronounced buckling of the array of MnO_6 octahedra in

the structure, with reduced Mn-O-Mn bond angles and a narrow e_g bandwidth.⁶ Preliminary studies have previously established that this compound is at the limit of the optimally doped manganites which exhibit a metal insulator transition at 63 K,⁸ and the value of the Curie temperature has been reported to be as low as 85 K.^{8,7} Therefore, this compound is likely to show the largest effects related to lattice distortion and magnetic disorder in any of the ferromagnetic mixed-valence manganese perovskites. The tolerance factor is almost the same as $(\text{Pr}_{0.7}\text{Ca}_{0.3})\text{MnO}_3$, which shows no metal-insulator transition in zero field.

II. EXPERIMENTAL RESULTS

The $(\text{Sm}_{0.65}\text{Sr}_{0.35})\text{MnO}_3$ sample was prepared by mixing high-purity oxide and carbonate powders. The mixture was repeatedly ground, pressed into a pellet, and annealed in air at 1200 °C until a single phase was obtained. X-ray diffraction showed a single phase that could be indexed on a cubic perovskite cell with $a_0 = 5.428 \text{ \AA}$. The density of the ceramic was 65% of the full x-ray density.

Magnetization, ac and dc susceptibility, and transport measurements have been performed on this sample. Magnetization was measured using a vibrating sample magnetometer (VSM) with a 12 T superconducting magnet. The absolute ac susceptibility in SI units was measured on a bar-shaped sample in a concentric coil system; the dc susceptibility was measured using a superconducting quantum interference device (SQUID) and a high-temperature VSM. The resistivity and magnetoresistance data were obtained from four-point probe measurements with a dc current in an in-line configuration.

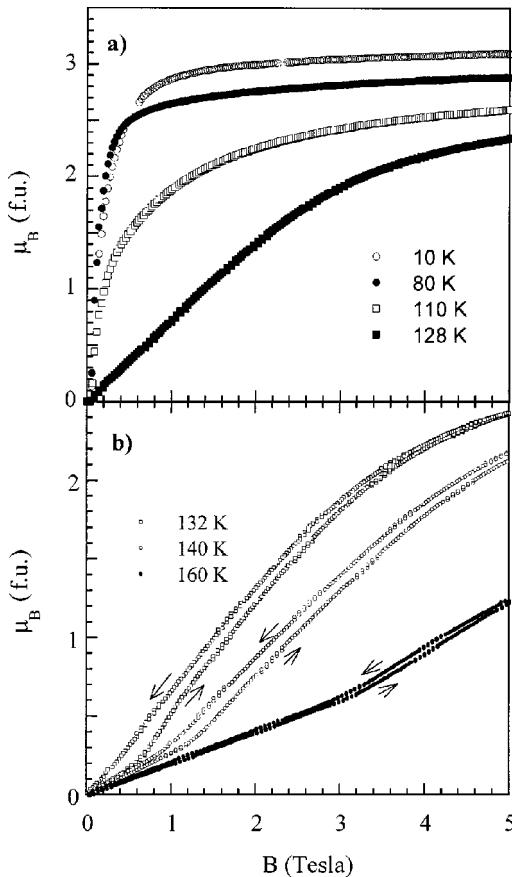


FIG. 1. (a) Magnetization curves below the Curie temperature. There is a crossover between the 10 and 80 K curves. (b) Magnetization curves above the Curie temperature. Note the sharp changes in the slope.

A. Low-temperature magnetic behavior

Magnetization curves below and near T_C are shown in Fig. 1(a). The data show that the magnetic order is essentially ferromagnetic. The zero-temperature moment of $(3.1 \pm 0.2)\mu_B$ per formula unit is to be compared with the manganese spin-only moment of $3.65\mu_B$ per formula unit. The full spin-only manganese moment is rarely achieved in ferromagnetic compounds of the type $(R_{1-x}A_x)\text{MnO}_3$ ($R = \text{La, Pr, Nd, Sm}$), which exhibit some degree of spin canting. The free ion moment of Sm^{3+} is $0.71\mu_B$, so that the contribution of the rare-earth ion is at most $0.25\mu_B$ per formula unit, which is less than 8% of the total magnetization. Similarly, $(\text{Sm}_{0.7}\text{Sr}_{0.3})\text{MnO}_3$ also exhibits a slightly reduced saturation moment, which, in addition to the marked decrease in low-temperature magnetization measured in applied fields of up to 1 T, has prompted speculation of antiferromagnetism or spin canting in this compound.⁷ Recent x-ray circular dichroism experiments carried out on the L_{III} edge of Sm^{3+} and K edge of Mn in $(\text{Sm}_{0.7}\text{Sr}_{0.3})\text{MnO}_3$ (Ref. 9) lend further support to the hypothesis that in this compound, the rare-earth ion is very weakly coupled to the manganese; the R and Mn moments tend to be aligned antiparallel in zero field and parallel in large applied fields.¹⁰ These compounds have a tendency to adopt randomly canted spin structures, becoming essentially antiferromagnetic in the limits $x=0$ and $x=0.5$.

The real component of the ac susceptibility (Fig. 2) shows three features: a rapid increase from 10 to 30 K, which

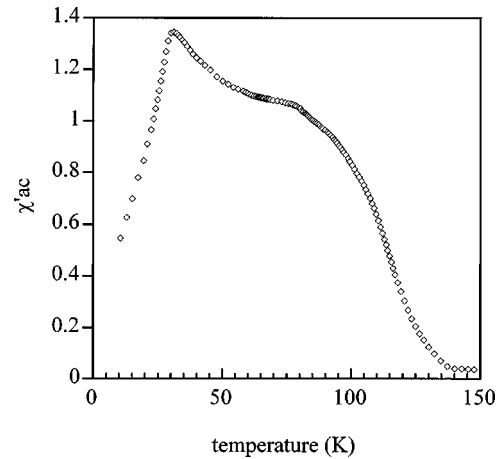


FIG. 2. Low-temperature dimensionless susceptibility (measured at 1 kHz under 80 A/m). There is no frequency dependence in the range (10 Hz to 1 kHz).

ends at a marked peak, a plateau from 40 to 80 K, and a gradual decrease between 80 and 140 K. The low-field dc magnetization exhibits similar features. There is no discontinuity, such as would be expected for a first-order magnetic phase transition. From the inverse susceptibility plot [Fig. 3(a)], it can be seen that $1/\chi$ extrapolates to zero at $T_C = 122$ K on cooling and at $T_C = 130$ K on heating. The Curie temperature of this material is not well defined, but the magnetic ordering transition falls in the range 120–130 K depending on the conditions of the measurement. Another feature to be noted is that the hysteresis of 8 K observed around T_C between field-cooling and zero-field-cooled-field-heating measurements does not depend on the applied field in the range 250 A/m to 3 kA/m.

The fall in the susceptibility below 30 K observed in these small applied fields is attributed here to the development of coercivity.

B. High-temperature magnetic behavior

Figure 3(b) shows the inverse susceptibility in the temperature range 100–600 K. Above 150 K, data measured in a dc field (250 A/m) and ac field (80 A/m, 1 kHz) are in very good agreement. However, it has to be noted that the inverse susceptibility curve does not exhibit the slope expected for a Curie-Weiss law for free manganese moments ($C=0.97$). This slope is only reached for temperatures higher than 400 K with a value of $\theta_p = 272$ K. The measured inverse susceptibility slope from 140 to 200 K gives the much higher value $C = 3.1 \pm 0.1$ and an intercept at $\theta_p = 90$ K. The contribution of Sm^{3+} to the susceptibility may be neglected, since it will be Curie-Weiss-like with $\theta_p \approx 0$.

C. Field-induced transition

Magnetization curves in the paramagnetic state are shown in Fig. 1(b). These curves show a very unusual field-induced change of slope which is not observed in the $(\text{Sm}_{0.7}\text{Sr}_{0.3})\text{MnO}_3$ compound. In the low-field regime the magnetization varies linearly with field, but above a critical field, which we denote as B_t , there is a more rapid increase in magnetization. These curves also show some hysteresis in

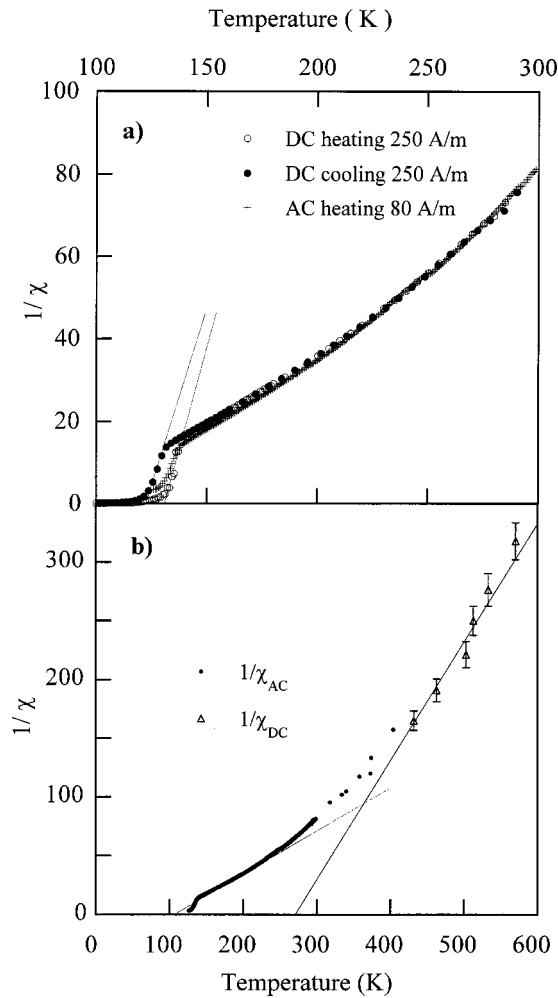


FIG. 3. (a) Inverse magnetic susceptibility above the Curie temperature: dc SQUID measurement under 250 A/m: field heating (open circles), field cooling (solid circles), ac susceptibility measurement under 80 A/m field heating (crosses). (b) High-temperature inverse susceptibility (triangles) and theoretical Curie-Weiss law (straight line) corresponding to free manganese ions. The adjusted Curie constant is 0.95, which is close to the theoretical value of 1. The straight line fitting the low-temperature part (140–200 K) corresponds to the value of $C=3.1$.

the range 130–160 K, which becomes negligible at higher temperatures. The corresponding variation of the critical field B_t as a function of temperature is plotted in Fig. 4. The variation of the critical field in the decreasing field measurement varies linearly with temperature from 130 K up to 200 K and goes to zero near the magnetic ordering temperature. However, the critical field for the increasing field measurements does not reach zero at the ordering temperature.

D. Transport properties

The resistivity (Fig. 5) shows a metal-insulator transition typical of manganites with a low Curie point. Here, again, as in the magnetic measurements, one can observe thermal hysteresis of 8 K between the cooling and heating curves. This is comparable to a hysteresis of 10 K measured in $(\text{Sm}_{0.7}\text{Sr}_{0.3})\text{MnO}_3$. The resistivity reaches a maximum at $T_p = 105$ K on cooling and at $T_p = 120$ K on heating. These values are below the values of T_C measured in the same condi-

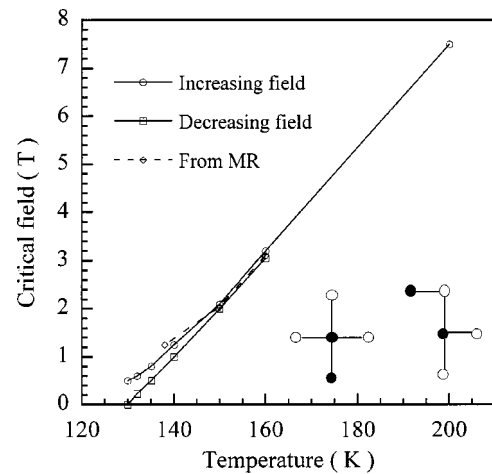


FIG. 4. Critical field B_t inducing the transition above the Curie temperature, deduced from the magnetization curves the field increasing (circles), B_t deduced from the magnetization curve with the field decreasing (squares), and B_t deduced from the magnetoresistance curves (lozenges). Two possible configurations of the five manganese clusters are shown in the figure where the solid circles represent the Mn^{4+} ions and the open circles the Mn^{3+} ions.

tions, but it is often observed that $T_p < T_C$ in the manganites. The cooling and heating resistivity curves at high temperature (130–300 K) can be very well fitted using the variable-range hopping model (see inset in Fig. 5):

$$\rho = \rho_\infty \exp\left(\frac{T_0}{T}\right)^{1/4}.$$

The value of $T_0^{1/4}$ deduced from the fit is 105 $\text{K}^{1/4}$ upon cooling and 120 $\text{K}^{1/4}$ upon heating, which agrees with values measured on similar compounds.¹¹ Neither a purely activated law $\rho = \rho_\infty \exp(T_0/T)$ nor the simple hopping law $\rho = \rho_0 T \exp(E_0/kT)$ is able to fit the data as well.^{12–14}

Above T_C there are two magnetoresistance regimes; at low fields, the resistance variation is initially quadratic with the field, as expected in the paramagnetic state. However, above a certain critical field, the magnetoresistance variation becomes linear, which is the behavior usually associated

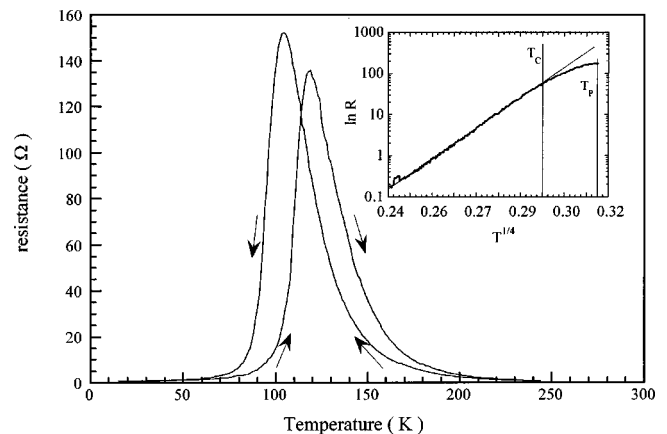


FIG. 5. Resistivity as a function of temperature under zero field showing hysteresis near T_C and fit assuming a variable-range hopping type conduction above the Curie temperature for the cooling curve (inset).

TABLE I. Calculated values of S , p_{eff}^2 and C for clusters with different sizes and with different ionic compositions.

Mn ions in cluster	Mn ³⁺ /Mn ⁴⁺	S	p_{eff}^2	C
1	1/0	24	24	1.10
1	0/1	15	15	0.69
4	3/1	15/2	255	2.39
4	2/2	7	224	1.81
5	3/2	9	360	2.90
5	2/3	17/2	322	1.72
6	3/3	21/2	483	2.59
6	4/2	11	528	3.95

with the ferromagnetic state of manganites. The critical field deduced from these magnetoresistance measurements is in good agreement with the critical field deduced from the magnetization curves (Fig. 4). We therefore associate the change in the magnetoresistance from quadratic to linear with the change in the magnetic state of the material in the paramagnetic region above the critical field B_t .

III. DISCUSSION

The (Sm_{0.65}Sr_{0.35})MnO₃ compound differs from a normal ferromagnetic manganite in two important aspects: (i) there is a field-induced transition at B_t in the paramagnetic state, and (ii) there is thermal hysteresis around T_C . We discuss each feature in turn.

A. Field-induced transition

The high value of the Curie constant just above T_C ($C = 3.1$) means that the effective moment is larger than that expected from the paramagnetic susceptibility of free manganese ions ($C = 0.97$). This suggests the presence of magnetic clusters. As the temperature increases, the size of the clusters decreases, and by 500 K, where the Curie constant has reached a value of 1.0 [Fig. 3(b)], the clusters have disappeared.

The effective Bohr magneton number p_{eff} is defined for $3d$ ions as $p_{\text{eff}} = g\sqrt{S(S+1)}$, where g is the Landé factor and S is the spin angular momentum quantum number. The Curie constant is given by $C = N\mu_0\mu_B^2 p_{\text{eff}}^2 / 3k$, where N is the total number of paramagnetic entities per cubic meter. In (Sm_{0.65}Sr_{0.35})MnO₃, there are three different magnetic ions Mn³⁺, Mn⁴⁺, and Sm³⁺. For Mn³⁺ and Mn⁴⁺, spin-only moments are given by $g = 2$ and $S = 2$ or $S = 3/2$. Values of p_{eff}^2 are equal to 24.0 and 15.0, respectively. For the Sm³⁺ ion, $p_{\text{eff}}^2 = 0.71$; its contribution represents at most 2% of the total Curie constant and can be neglected. The average value of p_{eff} for free paramagnetic Mn ions is equal to $\sqrt{\langle p_{\text{eff}}^2 \rangle} = 4.57$, which gives an average Curie constant of 0.97 and an expected slope of 1.03 in the $1/\chi$ vs T dependence.

Some possible clusters of Mn³⁺ and Mn⁴⁺ together with values of C are shown in Table I. A five-cluster (Mn₃³⁺Mn₂⁴⁺) with $p_{\text{eff}}^2 = 360$ comes closer to the observed value of C , but we expect there will be some distribution of cluster size and composition to satisfy the electron stoichiometry. We are assuming that the five manganese spins in

the cluster are strongly coupled in the temperature interval 130–160 K where C is determined. This is supported by the value of $\theta_p = 270$ K extrapolated from the high-temperature susceptibility.

In this picture, a cluster is formed by five Mn⁴⁺ ions sharing three electrons between them. Inside the clusters there is a large ferromagnetic coupling, whereas the interaction between clusters is rather small ($\theta_p = 87$ K). A few possible configurations for a five-manganese cluster are shown in Fig. 4. Since small ferromagnetic regions embedded in a low-density paramagnetic background of Mn³⁺ are similar to the spin polaron picture discussed in the recent literature,^{15–17} a possible correlation exists between the two concepts. While the electrons are delocalized inside the cluster, the electrical transport is dominated by the process of electrons hopping from cluster to cluster. Recent work by Ziese and Srinithiwarawong¹⁸ relates variable-range hopping (VRH) in polycrystalline manganite films to a defective microstructure. VRH behavior is thus attributed to nonstoichiometric regions or tunneling processes across grain boundaries. A possible source of clustering is local variation of the potential experienced by electrons in the Mn e_g^\uparrow band due to charge and structural fluctuations associated with the inhomogeneous Sr distribution in this compound. Thus the observed VRH behavior lends support to the cited work¹⁸. Arovas *et al.*¹⁹ have recently shown that systems described by double exchange are unstable towards phase separation near T_C . This was found for a doping range between 0.8 and 1, but the effect of finite fields is yet to be taken into account.

B. Hysteretic behavior

The field-induced transition in the paramagnetic state at B_t exhibits hysteresis when the temperature is near T_C and is continuous; therefore, it cannot correspond to an abrupt change in the nature of the clusters. We suppose that B_t must be the onset of a two-phase region where the five-Mn clusters coexist with larger ones; the five-Mn clusters are the α phase, the larger are the β phase, and, for a region of field for $B > B_t$, α and β coexist. In order to characterize the β phase, we need to look at its behavior in high fields where the magnetization curve is reversible. Figure 6(a) shows that the $M(B)$ data at different temperatures can be scaled by plotting them against $B/(T - \theta_p)$ where $\theta_p = 112$ K. The properties of the β phase are deduced by fitting a Langevin function to the high-field plot. The best fit is obtained for $m = 33\mu_B$. For comparison, the low-field part is fitted by a Langevin function with $m = 15\mu_B$, which agrees quite well with the result that $S = 9$ deduced from the Curie law. The clusters in the β phase are about twice as large as in the α phase, and the interaction between them represented by $\theta_p = 112$ K is a bit larger than that in the α phase ($\theta_p = 87$ K). In increasing the field up to B_t , the interaction between the clusters is given by $J_a \vec{s}_1 \cdot \vec{s}_2$, \vec{s}_1 and \vec{s}_2 being the spin of the clusters. J_a is equal to 0.05 K. At the critical field there is a sudden increase in the size and strength of the coupling between the clusters. The new interaction is given by $J_b \vec{S}_1 \cdot \vec{S}_2$ with J_b equal to 0.1 K. Since the interaction in play as well as the interacting entities are different above and below B_t , it is natural to observe hysteresis.

Hysteresis is already present in the paramagnetic state, just above T_C , and persists up to about 150 K. It suggests

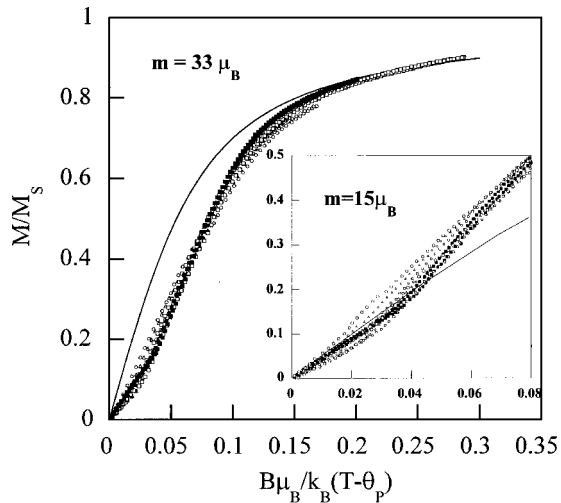


FIG. 6. Scaled M vs B curves fitted with the Langevin function both for high- and low-field parts.

that there is some difficulty in nucleating the α phase near T_C , and the α - β interfaces tend to be pinned.

The hysteresis at T_C would normally suggest a first-order magnetic phase transition, but we have found no evidence for any discontinuity of magnetization at T_C in $M(T)$ curves. We note, however, that the onset of the α - β transition occurs above a critical value of the magnetization, which is approximately 15% of the saturation magnetization. When approached from $T > T_C$ the ferromagnetic phase forms by interaction and alignment of the moments of five-Mn clusters of the α phase. However, when approached from $T < T_C$ the manganite reaches the paramagnetic state through disordering the clusters of the β phase, which are more strongly coupled and therefore lead to a higher value of T_C . We

therefore consider the field hysteresis in the paramagnetic state and the thermal hysteresis around T_C to be closely related.

However, the thermal hysteresis of magnetization and resistivity are somewhat different; the point of inflection in the resistivity measurement corresponds approximately to the magnetic transition. This is further evidence against a first-order magnetic phase transition. In manganites a small change in the magnetization can have a drastic effect on the resistivity—this is the so-called colossal magnetoresistance.

It has been shown that grain boundaries have a great influence on magnetoresistance.²⁰ Here it may be that the interfaces between the α and β phases behave like magnetic grain boundaries. The resistivity is greatest about 20 K below T_C where fluctuations in magnetization direction are most effective at inhibiting intercluster hopping.

IV. CONCLUSION

We have discovered a field-induced transition in the paramagnetic state of a ferromagnetic mixed-valence manganite, where the size of the basic magnetic entities increases from 5-Mn clusters with a moment of $\sim 13\mu_B$ to larger clusters with $m \sim 33\mu_B$. This clustering corresponds to electronic phase segregation, and the hysteresis observed as a function of temperature or applied field is related to the presence of an electronic two-phase region.

ACKNOWLEDGMENTS

This study forms part of the work of the OXSEN network, a program for Training and Mobility of Researchers supported by the European Union. It was partly supported by the U.S. Navy; N00014-97-1-0166.

- ¹R. von Helmholt, J. Wecker, B. Holzapfel, L. Shultz, and K. Samwer, *Phys. Rev. Lett.* **71**, 2331 (1993).
- ²S. von Molnar and J. M. D. Coey, *Curr. Opin. Solid State Mater. Sci.* **3**, 171 (1998).
- ³J. M. de Teresa, M. R. Ibarra, P. A. Algarabel, C. Ritter, C. Marquina, J. Blasco, J. Garcia, A. del Moral, and Z. Arnold, *Nature (London)* **386**, 256 (1997).
- ⁴G. Jakob, W. Westerburg, F. Martin, and H. Adrian, *Phys. Rev. B* **58**, 14 966 (1998).
- ⁵M. Fiebig, K. Miyano, Y. Tomioka, and Y. Tokura, *Science* **280**, 1925 (1998).
- ⁶H. Y. Hwang, S.-W. Cheong, P. G. Radaelli, M. Marezio, and B. Batlogg, *Phys. Rev. Lett.* **75**, 914 (1995).
- ⁷F. Damay, N. Nguyen, A. Maignan, M. Hervieu, and B. Raveau, *Solid State Commun.* **98**, 997 (1996).
- ⁸R. M. Thomas, L. Ranno, and J. M. D. Coey, *J. Appl. Phys.* **81**, 5763 (1997).
- ⁹R. M. Thomas, L. Ranno, and J. M. D. Coey (unpublished data).
- ¹⁰R. M. Thomas, V. Skumryev, J. M. D. Coey, and S. Wirth, *J. Appl. Phys.* **85**, 5384 (1999).
- ¹¹J. M. D. Coey, M. Viret, L. Ranno, and K. Ounadjela, *Phys. Rev. Lett.* **75**, 3910 (1995).
- ¹²G. J. Snyder, R. Hisker, S. Dicarolis, and S. Beasley, *Phys. Rev. B* **53**, 1 (1996).
- ¹³N. C. Yeh, R. Vasquez, D. Beam, and C. Fuc, *J. Phys.: Condens. Matter* **9**, 3713 (1996).
- ¹⁴N. C. Yeh, C. C. Fu, J. Y. T. Wei, R. P. Vasquez, J. Huynh, S. M. Maurer, G. Beach, and D. A. Beam, *J. Appl. Phys.* **81**, 5499 (1997).
- ¹⁵A. Lanzara, N. L. Saini, M. Brunelli, F. Natali, A. Bianconi, P. G. Radaelli, and S.-W. Cheong, *Phys. Rev. Lett.* **81**, 878 (1998).
- ¹⁶S. Yoon, H. L. Liu, G. Schollerer, S. L. Cooper, P. D. Han, D. A. Payne, S.-W. Cheong, and Z. Fisk, *Phys. Rev. B* **58**, 2795 (1998).
- ¹⁷M. R. Ibarra and J. M. De Teresa, *J. Magn. Magn. Mater.* **177-181**, 846 (1998).
- ¹⁸M. Ziese and C. Srinithiwarawong, *Phys. Rev. B* **58**, 11 519 (1998).
- ¹⁹D. P. Arovas, G. Gómez-Santos, and F. Guinea, *Phys. Rev. B* **59**, 13 569 (1999).
- ²⁰N. D. Mathur, G. Burnell, S. P. Isaac, T. J. Jackson, B.-S. Ted, J. L. MacManus-Driscoll, L. F. Cohen, J. E. Evetts, and M. G. Blamire, *Nature (London)* **387**, 266 (1997).